Sox10 mutation disrupts neural crest development in *Dom* Hirschsprung mouse model

E. Michelle Southard-Smith, Lidia Kos & William J. Pavan

Hirschsprung disease (HSCR, MIM #142623) is a multigenic neurocristopathy (neural crest disorder) characterized by absence of enteric ganglia in a variable portion of the distal colon. Subsets of HSCR individuals also present with neural crest-derived melanocyte deficiencies (Hirschsprung-Waardenburg, HSCR-WS, MIM #277580). Murine models have been instrumental in the identification and analysis of HSCR disease genes. These include mice with deficiencies of endothelin B receptor (*Ednrb*$^{s-l}$; refs 1,2) endothelin 3 (*Edn3*^{ls}; refs 1,3) the tyrosine kinase receptor *cRet*[4] and glial-derived neurotrophic factor[5–7]. Another mouse model of HSCR disease, *Dom*, arose spontaneously at the Jackson Laboratory[8]. While *Dom*/+ heterozygous mice display regional deficiencies of neural crest-derived enteric ganglia in the distal colon, *Dom/Dom* homozygous animals are embryonic lethal[8]. We have determined that premature termination of Sox10, a member of the *SRY*-like HMG box family of transcription factors, is responsible for absence of the neural crest derivatives in *Dom* mice. We demonstrate expression of *Sox10* in normal neural crest cells, disrupted expression of both *Sox10* and the HSCR disease gene *Ednrb* in *Dom* mutant embryos, and loss of neural crest derivatives due to apoptosis. Our studies suggest that *Sox10* is essential for proper peripheral nervous system development. We propose *SOX10* as a candidate disease gene for individuals with HSCR whose disease does not have an identified genetic origin.

We have pursued a positional cloning strategy to identify the molecular defect in *Dom* mice. Linkage analysis indicated the mutation arose in the C57BL/6J allele on mouse chromosome 15 (refs 8–10). High-resolution linkage analysis based on 1,716 meioses was used to narrow the *Dom* critical interval to a 0.1 cM region (Fig. 1*a*). Microsatellite and BAC-derived markers were used to establish a physical contig including a 167-kb BAC (43P19) containing the entire *Dom* critical interval (Fig. 1*b*). BLAST alignment of random sequences obtained from BAC 43P19 identified similarities to portions of several genes and ESTs (Fig. 1*c*). One candidate 3.1-kb transcript derived from these sequences is denoted *Sox10* on the basis of its homology with the 163-bp sequence entry of the *Sry*-type HMG box transcription factor *Sox10* (refs 11,12). Our *Sox10* cDNA sequence also demonstrated identity to a 3′ PCR product derived from RNA in K-1735 murine melanoma cells[13,14]. Consistent with its expression in K-1735 melanoma, *Sox10* transcripts were detected in melanocyte derived Melan-*a* cells[15] (northern-analysis data not shown) and in numerous other neural crest derivatives by *in situ* hybridization (Fig. 2). These included cranial, dorsal root, sympathetic and enteric ganglia and cells positioned in the dorsolateral migratory pathway (putative melanoblasts; Fig. 2). Given the correlation of *Sox10* expression with the two principal cell types affected in *Dom*/+ mice, neural crest-derived melanocytes and enteric ganglia, *Sox10* was assessed as a candidate gene for the *Dom* locus.

Northern-blot comparisons of wild-type (WT) and mutant samples revealed striking discrepancies in the level of *Sox10* steady-state mRNA (Fig. 3*a*). *Dom/Dom* embryos demonstrated a decreased intensity of *Sox10* mRNA. *Dom*/+ embryos demonstrated an apparent increased intensity that was not consistently observed amoung individual embryos from separate litters. To determine whether the altered expression was a primary defect in the *Sox10* gene or secondary to the neurocristopathy observed in affected embryos, we examined the *Sox10* cDNA sequence. The *Dom* mutation arose in the C57BL/6J allele of C57BL/6J X C3HeB/FeJLe-*a/a bc*/+ hybrid mice[8] and has subsequently been maintained on these inbred strains. Therefore, a genomic difference between *Dom* and C57BL/6J is likely to be the cause of the neural crest defects. Sequence comparisons with C57BL/6J *Sox10* cDNA revealed an extra guanine residue at nucleotide 929 only in the *Dom* allele (Fig. 3*b*). This is predicted to result in a translation frameshift in the putative *Sox10* open reading frame (ORF), generating 99 novel amino acids before a translation termination signal (Fig. 3*c*). These findings suggest that the single nucleotide insertion in the *Sox10* locus of *Dom* mice (now denoted *Sox10*^{Dom}) is responsible for this neurocristopathy.

Overlapping expression patterns of *Sox10* and the HSCR disease gene *Ednrb* (Figs 2,4; manuscript in preparation) in neural crest derivatives, and the requirement of endothelin signalling for neural crest development[3,16–20], prompted investigation of *Ednrb* expression in *Sox10*^{Dom} mutant embryos. Although *Ednrb*+ cells were detected in migrating neural crest cells of 10.5-d.p.c.

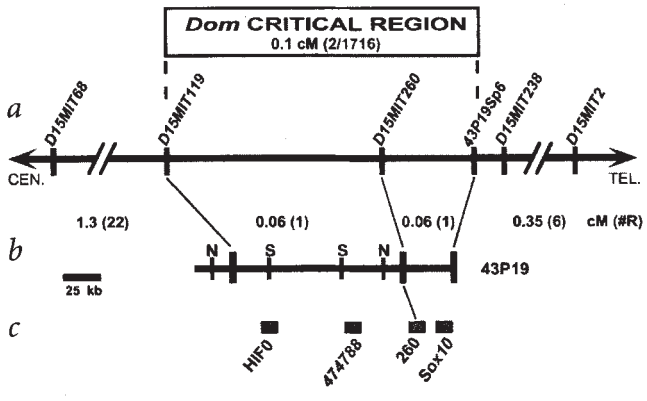

Fig. 1 Summary of *Dom* positional cloning strategy. ***a***, Resolution of the 0.1-cM genetic interval using 1,716 informative meioses is shown. Genetic distance between polymorphic markers (below line) is in centimorgans (cM) and number of recombinants (#R). ***b***, A 175-kb BAC clone (43P19), identified by PCR and hybridization screening of an arrayed mouse BAC library (Research Genetics) with *D15MIT119*, constitutes the entire *Dom* critical region. The relative positions of *Not*I (N) and *Sal*I (S) sites and genetic markers are indicated. *43P19Sp6* is a polymorphic BAC end-derived marker. ***c***, Approximate location of four candidate transcripts identified by single-pass sequencing. Histone 1(O) (*H1F0*), EST *474788*, EST*260* and *Sox10*.

Mouse Embryology Section, Building 49, Room 4A82, Laboratory of Genetic Disease Research, National Human Genome Research Institute, National Institutes of Health, 49 Convent Drive MSC 4472, Bethesda, Maryland 20892-4472, USA. Correspondence should be addressed to W.J.P. e-mail: bpavan@nhgri.nih.gov

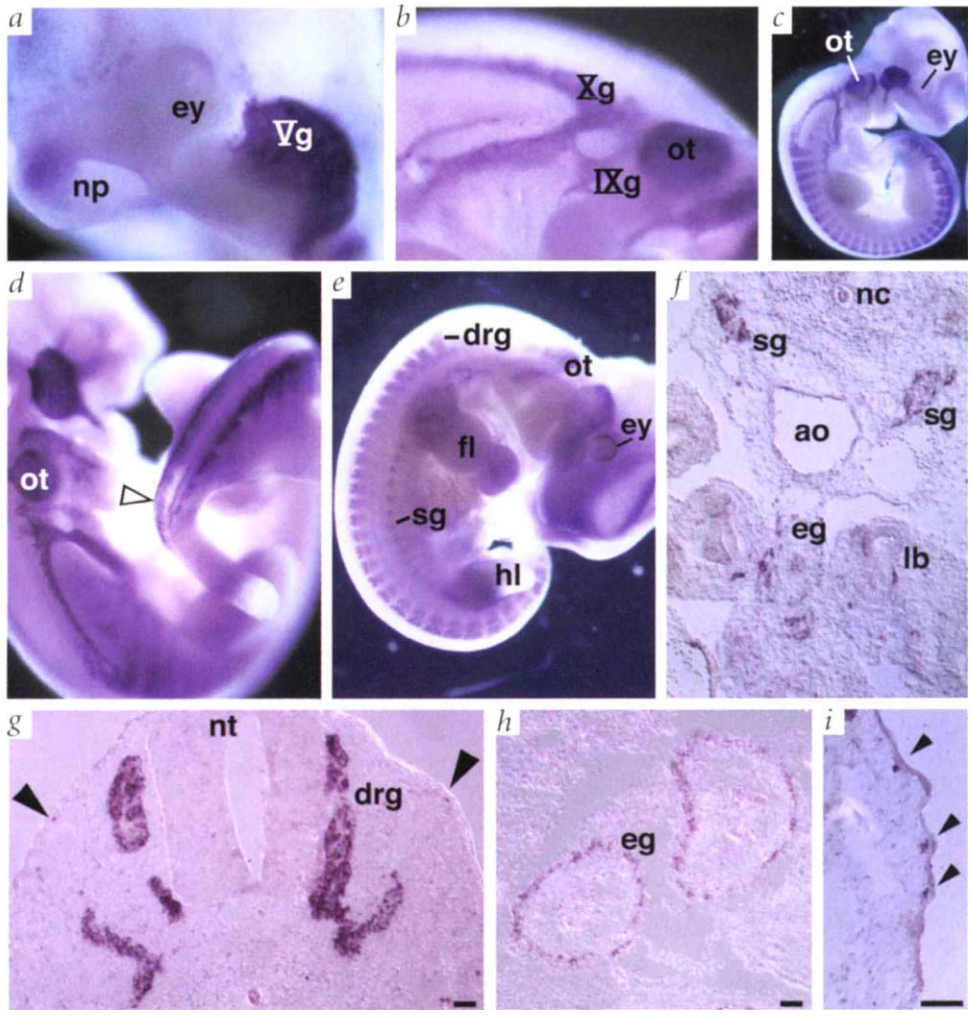

Fig. 2 *In situ* hybridization in WT embryos reveals extensive *Sox10* expression in migrating neural crest derivatives. Mouse embryos at 9.5-days-post-coitus (d.p.c.) demonstrating expression in cranial ganglia (***a***) V (***b***), X and IX and in areas consistent with locations of migrating neural crest (open arrow). ***c***, Extensive *Sox10* expression in peripheral nervous-system derivatives and otocyst (ot). ***d***, Migrating sacral neural crest in the tail of 10.5-d.p.c. mouse embryo. ***e***, *Sox10* is expressed in cranial, dorsal root (drg) and sympathetic ganglia (sg) of 11.5-d.p.c. mouse embryo. *In situ* hybridization of cross-sections in the trunk region of 12.5-d.p.c. mouse embryos show expression of *Sox10* in (***f***) sympathetic and enteric (eg) and (***g***) dorsal root ganglia and presumptive melanoblasts (solid arrows) and (***h***) the gut consistent with location of myenteric ganglia. ***i***, Higher magnification lateral to the neural tube demonstrates $Sox10^{+}$ cells in a location consistent with the dorsolateral melanoblast migratory pathway. Nasal pit (np), eye (ey), forelimb (fl), hindlimb (hl), notochord (no), dorsal aorta (ao), lung bud (lb), neural tube (nt). Size bar = 50 μm.

$Sox10^{Dom}/Sox10^{Dom}$ and $Sox10^{Dom}/+$ embryos, the cells were developmentally delayed in their migratory pathway (Fig. 4*a–c*). The neural crest defects became more apparent by 11.5 d.p.c., when *Ednrb* expression in the peripheral nervous system was almost completely absent in $Sox10^{Dom}/Sox10^{Dom}$ embryos and dramatically reduced in $Sox10^{Dom}/+$ embryos (Fig. 4*d–f*). The effect upon *Ednrb*+ cells, however, was spatially restricted, as the *Ednrb* expression in the marginal zone of the neural tube (a region with little observable *Sox10* expression) was not abolished by the $Sox10^{Dom}$ mutation (Fig. 4*g–i*). Examination of *Sox10* expression in the neural crest cells in mutant embryos revealed disruption of neural crest development (Fig. 5*a*). At 9.5 d.p.c., expression of *Sox10* was apparent in newly forming neural crest cells in both wildtype and $Sox10^{Dom}/Sox10^{Dom}$ embryos (data not shown). At 10.5 d.p.c., however, expression of *Sox10* in cranial ganglia was drastically reduced in $Sox10^{Dom}/Sox10^{Dom}$ embryos (Fig. 5*a*), whereas the newly migrating cells in the caudal regions of the $Sox10^{Dom}/Sox10^{Dom}$ embryos demonstrated a similar alteration to that seen with *Ednrb* at 10.5 d.p.c. (Fig. 4*a–c*). By 11.5 d.p.c., *Sox10* expression was not detectable in $Sox10^{Dom}/Sox10^{Dom}$ embryos except in the most caudal neural crest cells of the tail (data not shown). Neural crest-derived melanocyte development was also disrupted, as indicated by the absence of detectable cells containing dopachrome tautomerase (Dct^{+}), an early melanoblast lineage marker[21,22] in 10.5 and 11.5 d.p.c. $Sox10^{Dom}/Sox10^{Dom}$ embryos (data not shown). The lack of *Ednrb*+, *Sox10*+ and *Dct*+ cells in $Sox10^{Dom}/Sox10^{Dom}$ embryos could be due to reduced expression or absence of distinct cell lineages. Our data support the latter theory because the dorsal root ganglia are smaller in $Sox10^{Dom}/Sox10^{Dom}$ embryos (Fig. 4*i*, neurofilament immunostaining, haematoxylin and eosin and methyl green staining; data not shown) and cells undergoing apoptosis are evident within migrating neural crest and dorsal root ganglia of mutant embryos (Fig. 5*b*).

The neurocristopathy observed in $Sox10^{Dom}$ mice, the spatiotemporal expression of *Sox10* within the peripheral nervous system and the altered expression patterns of *Ednrb*, $Sox10^{Dom}$ and *Dct* all support the role of *Sox10* as a key factor in neural crest development. The SOX family of transcription factors is defined by sequence similarity of its members to the HMG DNA-binding motif (SRY box) present in the mammalian sex-determining gene, *SRY*[23,24]. SOX proteins are thought to function as architectural transcriptional regulators by altering the physical proximity of *cis*-acting elements through DNA bending[23,24]. *Sox* genes have been identified in species as diverse as human and *Caenorhabditis elegans* and play critical roles in cell-fate determination during development[23–27]. SOX10 demonstrates highest homology with SOX9 in three domains: the HMG box, a short-segment N terminal to the HMG box and the putative transcription activation domain[28,29].

The single base insertion in $Sox10^{Dom}$ shifts the putative ORF C terminal to the HMG box. As a consequence, the N-terminal and DNA-binding domains are present, but the putative activation domain is replaced by 99 novel amino acids. Three inde-

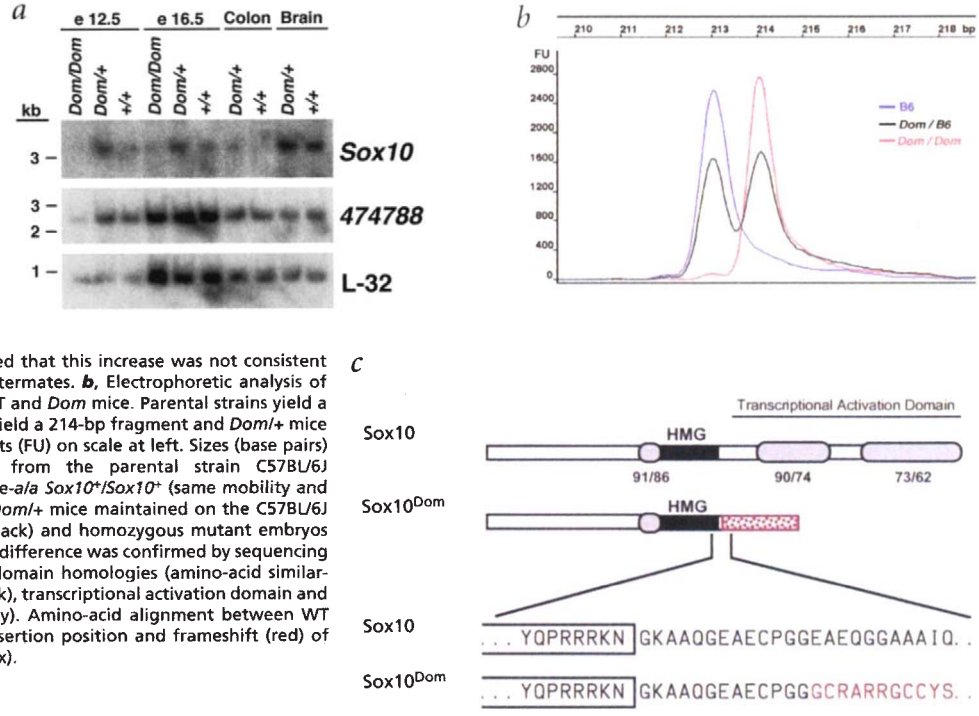

Fig. 3 Mutation of *Sox10* in *Dom* mice. ***a***, Altered *Sox10* expression in *Dom* tissues was identified by northern-blot analysis of polyA+ RNA from individual embryos at embryonic (e) days 12.5 and 16.5 p.c., adult colon and brain. Panels show autoradiographs after hybridization with a 2.7-kb *Sox10* cDNA clone (dcgs10-1), the 1.3-kb *Not*I–*Eco*RI fragment of Est *474788* and an RNA loading control, L-32 (ref. 33). Genotypes are indicated above each lane (*Dom/Dom*, homozygous mutant; *Dom/+*, heterozygous mutant; +/+, WT). Although heterozygotes appear to have an increased intensity of *Sox10* expression, additional northern analyses demonstrated that this increase was not consistent amoung four *Dom/+* 12.5-day-p.c. littermates. ***b***, Electrophoretic analysis of *Sox10* genomic PCR products from WT and *Dom* mice. Parental strains yield a 213-bp product, *Dom/Dom* embryos yield a 214-bp fragment and *Dom/+* mice yield both products. Fluorescence units (FU) on scale at left. Sizes (base pairs) at top of PCR products derived from the parental strain C57BL/6J *Sox10*+/*Sox10*+ (B6, blue) [C3HeB/FeJLe-*a*/*a* *Sox10*+/*Sox10*+ (same mobility and sequence as B6, not shown)], adult *Dom/+* mice maintained on the C57BL/6J strain background at N8 (*Dom/B6*, black) and homozygous mutant embryos (*Dom/Dom*, red). Single base pair size difference was confirmed by sequencing (data not shown). ***c***, Sox10 protein domain homologies (amino-acid similarity/identity) with Sox9. HMG box (black), transcriptional activation domain and N-terminal of the HMG domain (grey). Amino-acid alignment between WT and *Sox10*^{Dom} mutation depicting insertion position and frameshift (red) of protein sequence. HMG box (open box).

pendent modes of action can explain how the *Dom* neurocristopathy derives from this mutation. First, haploinsufficiency may result from the absence of a stable or a functional Sox10 protein. Second, if a stable protein product is made from the *Sox10*^{Dom} locus, the mutant domain could cause a dominant transcriptional activation of inappropriate genes in neural crest cells. Third, a dominant negative action caused by appropriate DNA binding without transcriptional transactivation might result in disruption of normal function. Premature truncation of SOX9 also results in a dominant human developmental disorder, campomelic dysplasia, apparently as a consequence of haploinsufficiency[28,29].

Sox10 and *Ednrb* exhibit overlapping patterns of expression in the embryonic peripheral nervous system (Figs 2,4). The reduced

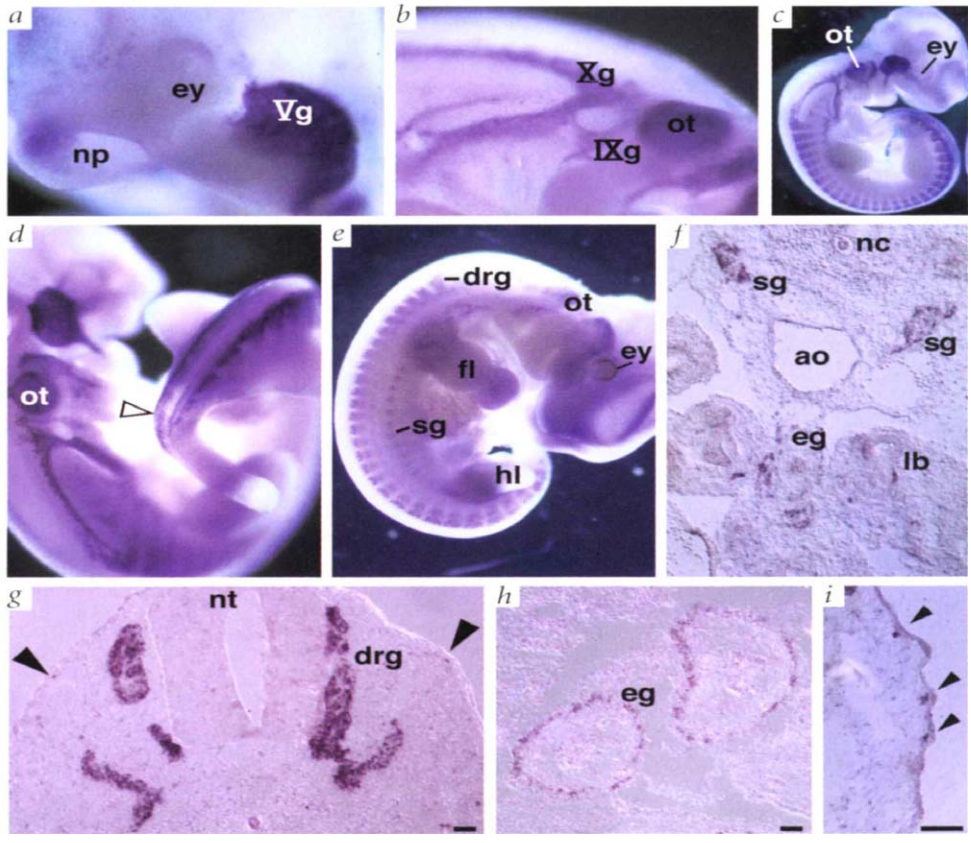

Fig. 4 Disrupted expression of *Ednrb* in *Sox10*^{Dom} mutants. Whole-mount (***a–f***) and trunk section (***g–i***) *in situ* hybridization of *Ednrb* in embryos at 10.5 (*a–c*), 11.5 (*d–f*) and 12.5 (*g–i*) d.p.c. WT embryos (*a,d,g*) show a neural crest expression pattern similar to that observed with *Sox10* (Fig. 2*c,e,g*). *Sox10*^{Dom}/+ (*b,e,h*) and *Sox10*^{Dom}/*Sox10*^{Dom} (*c,f,i*) embryos display mis-localized *Ednrb*+ cells along the neural crest migratory pathways at 10.5 d.p.c. (*b,c*). *Ednrb*+ cells were undetectable in the peripheral nervous system but were present in marginal zone of the neural tube (nt) of *Sox10*^{Dom}/*Sox10*^{Dom} embryos at 11.5 and 12.5 d.p.c. (*f,i*). Sympathetic ganglia (sg), dorsal root ganglia (drg), forelimb (fl).

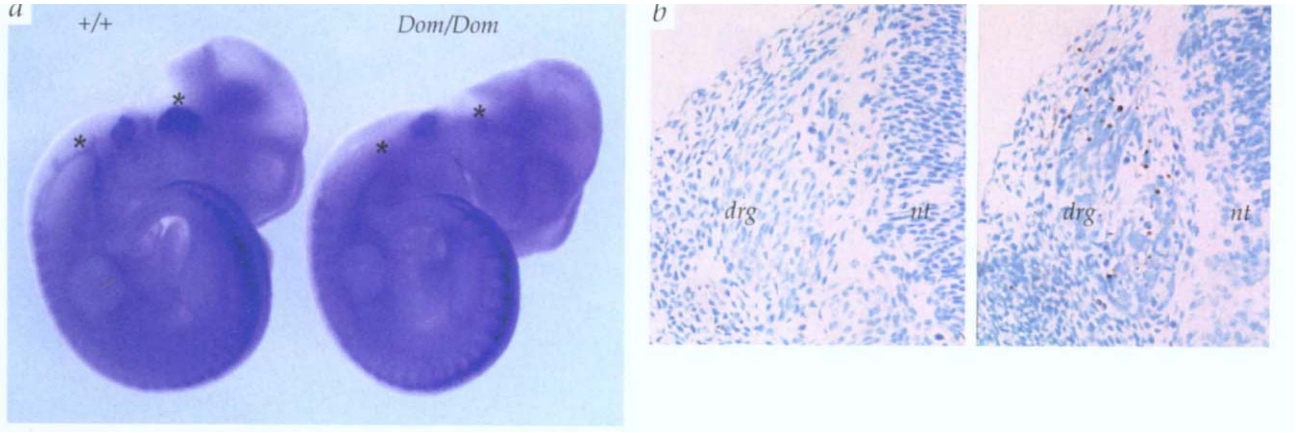

Fig. 5 Disrupted neural crest development and apoptosis in *Sox10*^{Dom} mutants. ***a***, Whole-mount *in situ* hybridization of 10.5-d.p.c. *Sox10*$^{+}$/*Sox10*$^{+}$ (left) and *Sox10*^{Dom}/*Sox10*^{Dom} (right) mouse embryos with *Sox10* probe. *Sox10*^{Dom}/*Sox10*^{Dom} embryos demonstrate a similar disruption of neural crest derivatives as seen with *Ednrb* expression. Expression in cranial ganglia is disrupted at this stage, whereas more caudal neural crest cells demonstrate delayed migration to the dorsal root ganglia. Cranial ganglia V and X are denoted by astericks. ***b***, The altered expression of neural crest markers is probably a consequence of apoptosis. Comparison of sections through *Sox10*$^{+}$/*Sox10*$^{+}$ (left panel), *Sox10*^{Dom}/*Sox10*$^{+}$ (right panel) and *Sox10*^{Dom}/*Sox10*^{Dom} (not shown) 11.5 d.p.c. embryos by TUNEL analysis demonstrated significant apoptosis (brown DAB precipitate) in migrating neural crest and dorsal root ganglia of mutant embryos.

Ednrb expression observed (Fig. 4) cannot account for all of the neural crest defects observed in *Dom* mice, as *Sox10*^{Dom}/*Sox10*^{Dom} embryos die *in utero*[8], whereas *Ednrb*$^{s-l}$/*Ednrb*$^{s-l}$ mice can survive past weaning and do not exhibit overt defects in cranial and dorsal root ganglia. Furthermore, embryological studies show that enteric-neuron colonization of the entire gut is retarded in *Sox10*^{Dom}/+ embryos from 11 d.p.c., in contrast to the later-onset and spatially restricted large-intestine deficiencies observed in *Ednrb*$^{s-l}$/*Ednrb*$^{s-l}$ embryos (12.5 d.p.c; refs 17,30). The expression of *Sox10* mRNA in migrating neural crest derivatives suggests a cell-autonomous role; experiments in aggregation chimaeras, however, suggest that *Dom* and *Ednrb/Edn3* mutations do not act in a strictly neuroblast-autonomous fashion[17,30–32]. Kapur *et al.* hypothesize that complex signalling between the migratory neural crest and the gut mesenchymal cells alters the microenvironment, ultimately influencing enteric ganglia formation[17]. Future studies will determine the genes regulated by SOX10 and their influence on the microenvironmental milieu.

The inheritance of HSCR in humans has been described as an autosomal dominant disorder with variable expressivity (MIM #142623). This is similar to the dominant action of *Sox10*^{Dom}, whose expressivity is influenced by genetic background[8]. Although there are no reports demonstrating linkage between HSCR with the human *SOX10* locus on 22q12–13 (data not shown), we propose that *SOX10* mutations will be responsible for phenocopies of HSCR, WS and other neural crest disorders. Moreover, identification of the downstream targets of *Sox10*, and the genes that modify the severity of the neurocristopathy in the *Sox10*^{Dom} HSCR mouse model, will provide additional insights into the genetic regulation of neural crest development.

Methods

Animal crosses. *Dom* arose and has been maintained on a C57BL/6J × C3HeB/FeJLe-*a/a* background. C57BL/6JLe × C3HeB/FeJLe-a/a *Dom*/+ mice were obtained from the Jackson laboratory and crossed to wild-derived (CAST/Ei and MOLF/Ei) strains. F1 mice displaying a ventral belly spot and white feet were selected for F1 backcrosses to C3HeB/FeJLe-a/a or used in intercrosses. A total of 308 mice were generated from intercrosses (616 informative meioses) and 1,100 animals were generated from backcross analyses. At weaning, animals were classified as +/+ or *Dom*/+ on the basis of the presence of a belly spot, white feet and white tail. (Note that *Dom/Dom* animals are embryonic lethal.) All progeny were typed[34] with *D15MIT68* and *D15MIT2* [http://www.genome.wi.mit.edu]. Recombinants were genotyped with *D15MIT119, D15MIT260, D15MIT238* and *43P19Sp6* and were then test-crossed to verify carrier status at the *Dom* locus. The critical recombinants used to define the *Dom* critical interval (animals 1903 and 2382) were both phenotypically *Dom*/+, and progeny from test crosses using these mice exhibited the *Dom*/+ phenotypes. For northern analysis, embryos were obtained from intercrosses of *Dom*/+ mice maintained on a C57BL/6J × C3HeBFeJLe-*a/a* background. Genotypes of individual embryos were determined from yolk-sac DNA with markers *D15MIT68* and *D15MIT71*. Total RNA was isolated with RNAzol (Tel-test) and oligo-dT selected on Oligotex minicolumns (Qiagen). Northern-blot analysis using 0.2–0.5 μg of polyA^{+} RNA was performed as described[35]. Animal care was in accordance with NIH guidelines.

cDNA isolation and mutation analysis. An M13 shotgun library was generated from BAC 43P19 DNA. Single-stranded clones (506) were partly sequenced by dye-primer chemistry (Amersham, ABI 377) and compared to available sequence databases. *Sox10* cDNA clones were isolated from a 10.5-d.p.c. C57Bl/6J embryo library (Genetrapper, Life Technologies) using oligonucleotides for capture (5′–GCGGCACGCAGAAAGCTAGCC–3′) and repair (5′–TACCCTCACCTCCACAATGCT–3′). Protein domains were analysed with BLAST (http://www.ncbi.nlm.nih.gov), ProDom BLASTP (http://protein.toulouse.inra.fr/prodom.html), GCG lite (http://molbio.info.nih.gov/molbio/gcglite/) and MacVector (International Biotechnologies) software. The putative open reading frame (ORF) begins at the first methionine of the largest ORF. Sequencing templates for mutation analysis were generated by RT-PCR of total RNA from C57BL/6J adult WT brain and *Dom/Dom* mutant embryos. PCR amplification of Sox10 sequences was achieved with two sets of oligonucleotides primers for the 5′ (capture oligo + 5′–CTGGGCTGCACACAGGAGATGG–3′) and 3′ (5′–GCTGTCCAGCCAGGGTGTTTGG–3′ + 5′–TCCTCAATGAAGGGGCGCTTG–3′) halves of the mRNA. PCR primers 6-FAM DCGS10BH2midFB (5′–AGGTTGCTGAACGAAAGTGACA–3′) and DCGS10BH2midRB (5′–GTCCAGGTGGGCACTCTTGTA–3′) flanking the insertion site were used to amplify the mutant region from WT and mutant genomic DNAs. Products were denatured and resolved by denaturing gel electrophresis on an ABI 377 Sequencer (Advanced Biotechnologies) sequencer). Image capture and analysis were performed with GENESCAN and GENOTYPER software packages (Advanced Biotechnologies).

***In situ* hybridization.** WT embryos were obtained from matings of C57Bl/6J mice (Fig. 2) or control littermates (Fig. 4). Noon of the plug day was considered 0.5 d.p.c. Non-radioactive whole mount and cryosection *in situ* hybridization was performed according to published protocols[36].

Digoxigenin antisense probes were made with templates: 1.5-kb *Sox10* (nucleotides 1287–2787, dcgs10-1 *Pvu*II T7 RNA polymerase); 0.96-kb *Ednrb* (nucleotides 555–1514, pWP40 *Kpn*I T7 RNA polymerase); 1.2-kb *Dct*[21]. TUNEL analysis was performed with the TdT Frag-EL kit (Oncogene) according to the manufacturer's protocol.

GenBank accession numbers. The accession number for *Sox10* for the full-length cDNA is AF017182; those for the HMG box region are U70441 & Z18959 and for the 3′ PCR product identified in differential display is D87031. Accession numbers relevent to the physical map of the Dom locus include those for the polymorphic BAC end-derived marker 43P19Sp6 (AF016235), histone 1(o) (H1FO) (U18295), the EST 474788 (AA038997), and the EST 260 (H32817). The accession number for the *Ednrb in situ* hybridization probe (base pairs 555–1514) is U32329.

Acknowledgements

We thank R. Nussbaum, L. Biesecker, A. Wynshaw-Boris, P. Schwartzberg and S. Loftus for critical reading of the manuscript; R. Kapur, J. Trent, H. Arnheiter and A. Chakravarti for discussions; J. Ellison for sequencing; E. Green, J. Touchman and A. Baxevanis for assistance with single pass-sequencing; K. Dunn for advice and assistance; J.R. Smith for image capture of genomic PCR on ABI gels; and D. Leja for graphics.

Received 25 September; accepted 25 November, 1997.

1. Lane, P.W. Association of megacolon with two recessive spotting genes in the mouse. *J. Hered.* **57**, 29–31 (1966).
2. Hosoda, K. *et al.* Targeted and natural (*piebald-lethal*) mutations of endothelin-B receptor gene produce megacolon associated with spotted coat color in mice. *Cell* **79**, 1267–1276 (1994).
3. Baynash, A.G. *et al.* Interaction of endothelin-3 with endothelin-B receptor is essential for development of epidermal melanocytes and enteric neurons. *Cell* **79**, 1277–1285 (1994).
4. Schuchardt, A., D'Agati, V., Larsson-Blomberg, L., Costantini, F. & Pachnis, V. Defects in the kidney and enteric nervous system of mice lacking the tyrosine kinase receptor Ret. *Nature* **367**, 380–383 (1994).
5. Sanchez, M.P. *et al.* Renal agenesis and the absence of enteric neurons in mice lacking GDNF. *Nature* **382**, 70–73 (1996).
6. Pichel, J.G. *et al.* Defects in enteric innervation and kidney development in mice lacking GDNF. *Nature* **382**, 73–76 (1996).
7. Moore, M.W. *et al.* Renal and neuronal abnormalities in mice lacking GDNF. *Nature* **382**, 76–79 (1996).
8. Lane, P.W. & Liu, H.M. Association of megacolon with a new dominant spotting gene (*Dom*) in the mouse. *J. Hered.* **75**, 435–439 (1984).
9. Pingault, V. *et al.* Human homology and candidate genes for the *Dominant megacolon* locus, a mouse model of Hirschsprung disease. *Genomics* **39**, 86–89 (1997).
10. Puliti, A. *et al.* A high-resolution genetic map of mouse chromosome 15 encompassing the *Dominant megacolon* (*Dom*) locus. *Mamm. Genome* **6**, 763–768 (1995).
11. Stock, D.W., Buchanan, A.V., Zhao, Z. & Weiss, K.M. Numerous members of the Sox family of HMG box-containing genes are expressed in developing mouse teeth. *Genomics* **37**, 234–237 (1996).
12. Wright, E.M., Snopek, B. & Koopman, P. Seven new members of the Sox gene family expressed during mouse development. *Nucleic Acids Res.* **21**, 744 (1993).
13. Tani, M. *et al.* Isolation of a novel Sry-related gene that is expressed in high-metastatic K-1735 murine melanoma cells. *Genomics* **39**, 30–37 (1997).
14. Hashimoto, Y. *et al.* Identification of genes differentially expressed in association with metastatic potential of K-1735 murine melanoma by messenger RNA differential display. *Cancer Res.* **56**, 5266–5271 (1996).
15. Bennett, D.C., Cooper, P.J. & Hart, I.R. A line of non-tumorigenic mouse melanocytes, syngeneic with the B16 melanoma and requiring a tumour promoter for growth. *Int. J. Cancer* **39**, 414–418 (1987).
16. Gershon, M.D. Neural crest development: do developing enteric neurons need endothelins? *Curr. Biol.* **5**, 601–604 (1995).
17. Kapur, R.P., Sweetser, D.A., Doggett, B., Siebert, J.R. & Palmiter, R.D. Intercellular signals downstream of endothelin receptor-B mediate colonization of the large intestine by enteric neuroblasts. *Development* **121**, 3787–3795 (1995).
18. Lahav, R., Ziller, C., Dupin, E. & Le Douarin, N.M. Endothelin 3 promotes neural crest cell proliferation and mediates a vast increase in melanocyte number in culture. *Proc. Natl. Acad. Sci. USA* **93**, 3892–3897 (1996).
19. Opdecamp, K. *et al.* Melanocyte development in vivo and in neural crest cell cultures: crucial dependence on the Mitf basic-helix-loop-helix-zipper transcription factor. *Development* **124**, 2377–2386 (1997).
20. Reid, K. *et al.* Multiple roles for endothelin in melanocyte development: regulation of progenitor number and stimulation of differentiation. *Development* **122**, 3911–3919 (1996).
21. Steel, K.P., Davidson, D.R. & Jackson, I.J. TRP-2/DT, a new early melanoblast marker, shows that steel growth factor (*c-kit* ligand) is a survival factor. *Development* **115**, 1111–1119 (1992).
22. Pavan, W.J. & Tilghman, S.M. *Piebald lethal* (s^l) acts early to disrupt the development of neural crest-derived melanocytes. *Proc. Natl. Acad. Sci. USA* **91**, 7159–7163 (1994).
23. Pevny, L.H. & Lovell-Badge, R. Sox genes find their feet. *Curr. Opin. Genet. Dev.* **7**, 338–344 (1997).
24. Prior, H.M. & Walter, M.A. SOX genes: architects of development. *Mol. Med.* **2**, 405–412 (1996).
25. Foster, J.W. *et al.* Campomelic dysplasia and autosomal sex reversal caused by mutations in an *SRY*-related gene. *Nature* **372**, 525–530 (1994).
26. Schilham, M.W., Moerer, P., Cumano, A. & Clevers, H.C. Sox-4 facilitates thymocyte differentiation. *Eur. J. Immunol.* **27**, 1292–1295 (1997).
27. Wagner, T. *et al.* Autosomal sex reversal and campomelic dysplasia are caused by mutations in and around the SRY-related gene SOX9. *Cell* **79**, 1111–1120 (1994).
28. Bell, D.M. *et al.* SOX9 directly regulates the type-II collagen gene. *Nature Genet.* **16**, 174–178 (1997).
29. Sudbeck, P., Schmitz, M.L., Baeuerle, P.A. & Scherer, G. Sex reversal by loss of the C-terminal transactivation domain of human SOX9. *Nature Genet.* **13**, 230–232 (1996).
30. Kapur, R.P. *et al.* Abnormal microenvironmental signals underlie intestinal aganglionosis in *Dominant megacolon* mutant mice. *Dev. Biol.* **174**, 360–369 (1996).
31. Kapur, R.P., Yost, C. & Palmiter, R.D. Aggregation chimeras demonstrate that the primary defect responsible for aganglionic megacolon in lethal spotted mice is not neuroblast autonomous. *Development* **117**, 993–999 (1993).
32. Rothman, T.P., Goldowitz, D. & Gershon, M.D. Inhibition of migration of neural crest-derived cells by the abnormal mesenchyme of the presumptive aganglionic bowel of *ls/ls* mice: analysis with aggregation and interspecies chimeras. *Dev. Biol.* **159**, 559–573 (1993).
33. Dudov, K.P. & Perry, R.P. The gene family encoding the mouse ribosomal protein L32 contains a uniquely expressed intron-containing gene and an unmutated processed gene. *Cell* **37**, 457–468 (1984).
34. Pavan, W.J., Mac, S., Cheng, M. & Tilghman, S.M. Quantitative trait loci that modify the severity of spotting in piebald mice. *Genome Res.* **5**, 29–41 (1995).
35. Swift, G.H., Dagorn, J.C., Ashley, P.L., Cummings, S.W. & MacDonald, R.J. Rat pancreatic kallikrein mRNA: nucleotide sequence and amino acid sequence of the encoded preproenzyme. *Proc. Natl. Acad. Sci. USA* **79**, 7263–7267 (1982).
36. Wilkinson, D.G. & Nieto, M.A. Detection of messenger RNA by in situ hybridization to tissue sections and whole mounts. *Methods Enzymol.* **225**, 361–373 (1993).